Lithuanian Journal of Physics, Vol. **44**, No. 6, pp. 439–446 (2004)

INFLUENCE OF CHEMICAL BONDS ON Bi AND Sb XPS SHIFTS IN Bi_2S_3 AND Sb_2S_3 CRYSTALS

V. Lazauskas [a], V. Nelkinas [a], and J. Grigas [b]

[a] *Vilnius Pedagogical University, Studentų 39, LT-08106 Vilnius, Lithuania*
[b] *Vilnius University, Saulėtekio 9, LT-10220 Vilnius, Lithuania*
E-mail: jonas.grigas@ff.vu.lt

Received 30 April 2004

Dedicated to the 100th anniversary of Professor A. Jucys

The paper presents the results of theoretical calculations of the shifts of Bi and Sb X-ray photoelectron spectra (XPS) due to chemical bond formation in Bi_2S_3 and Sb_2S_3 crystals. The energies of core levels of Bi, Sb, and S atoms are calculated by both the Hartree–Fock–Dirac (HFD) and Hartree–Fock methods and compared with the experimental values. The HFD method explains well the experimentally obtained spin–orbit splitting of the XPS. However, both theoretical methods give higher negative core level energies than their experimental values are.

Keywords: XPS, electronic structure, Bi_2S_3 and Sb_2S_3 crystals

PACS: 71.20.Ps, 79.60.Bm

1. Introduction

Bi_2S_3 and Sb_2S_3 are highly photoconductive materials promising for energy conservation applications. These crystals have a "friable" crystal lattice of complicated chemical bonding, which implies interesting electronic and lattice properties and causes weak phase transitions without change of symmetry [1]. For a review of the physical properties of these crystals see [2].

X-ray photoelectron spectra of Bi_2S_3 and Sb_2S_3 single crystals in the energy range of 0–1400 eV and over a wide temperature range have been studied in [3, 4]. Experimental energies of the valence band and core levels are compared with the results of theoretical *ab initio* calculations by the Hartree–Fock (HF) method of the molecular model of the crystals. However, the calculated energies are more negative by 10–50 eV than the experimental values. In addition, the HF method does not take into consideration the spin–orbit interaction. Therefore, it gives a mean value of energy independent of the spin. Meanwhile, the experimental data show that the X-ray photoelectron spectra (XPS) of core levels always split into spin–orbit doublets.

The aim of this work is to evaluate the splitting of the spin–orbit doublets of the XPS by the Hartree–Fock–Dirac (HFD) method and to compare the results with the experimental energies and the ones calculated by the HF method.

2. The Hartree–Fock–Dirac equations

The Hartree–Fock–Dirac single-electron equation [5] is given by

$$\left(h^{\mathrm{D}} + \sum_j (J_j - K_j)\right)\varphi_i = \varepsilon_i \varphi_i, \qquad (1)$$

where

$$h^{\mathrm{D}} = c\,\vec{\alpha}\cdot\vec{p} + \beta mc^2 + V_i, \quad V_i = -\frac{e^2 Z}{r_i}, \qquad (2)$$

is the operator of the single-electron kinetic energy and interaction with the electrostatic field (m is the rest mass of the electron, e is the charge, c is the speed of light) and ε_i is the energy state of the ith electron, r_i is the electron distance from the nucleus. Here

$$\vec{\alpha}\cdot\vec{p} = \alpha_x p_x + \alpha_y p_y + \alpha_z p_z \qquad (3)$$

is the scalar product of the momentum operator

$$\vec{p} = -\mathrm{i}\hbar\left(\frac{\partial}{\partial x}\vec{i} + \frac{\partial}{\partial y}\vec{j} + \frac{\partial}{\partial z}\vec{k}\right)$$

ISSN 1648-8504

with the four-dimensional Dirac matrices:

$$\alpha_x = \begin{pmatrix} 0_2 & \sigma_x \\ \sigma_x & 0_2 \end{pmatrix}, \quad \alpha_y = \begin{pmatrix} 0_2 & \sigma_y \\ \sigma_y & 0_2 \end{pmatrix}, \quad \alpha_z = \begin{pmatrix} 0_2 & \sigma_z \\ \sigma_z & 0_2 \end{pmatrix}, \quad \beta = \begin{pmatrix} I_2 & 0_2 \\ 0_2 & -I_2 \end{pmatrix}; \tag{4}$$

$$\sigma_x = \begin{pmatrix} 0 & 1 \\ 1 & 0 \end{pmatrix}, \quad \sigma_y = \begin{pmatrix} 0 & -\mathrm{i} \\ \mathrm{i} & 0 \end{pmatrix}, \quad \sigma_z = \begin{pmatrix} 1 & 0 \\ 0 & -1 \end{pmatrix}, \quad I_2 = \begin{pmatrix} 1 & 0 \\ 0 & 1 \end{pmatrix}, \quad 0_2 = \begin{pmatrix} 0 & 0 \\ 0 & 0 \end{pmatrix}. \tag{5}$$

Two-electron Coulomb (J_j) and exchange (K_j) interaction operators in Eq. (1) are given by the following relations:

$$J_j|\varphi_q\rangle = \int \varphi_j^*(r_2) g_{12} \varphi_j(r_2)\,\mathrm{d}r_2 |\varphi_q\rangle, \tag{6}$$

$$K_j|\varphi_q\rangle = \int \varphi_j^*(r_2) g_{12} \varphi_q(r_2)\,\mathrm{d}r_2 |\varphi_j\rangle. \tag{7}$$

The matrix elements of these operators are two-electron integrals:

$$\begin{aligned} &\langle\varphi_p|J_j|\varphi_q\rangle \\ &\quad = \iint \varphi_p^*(r_1)\varphi_j^*(r_2) g_{12} \varphi_q(r_1)\varphi_j(r_2)\,\mathrm{d}r_1\,\mathrm{d}r_2 \\ &\quad = \langle\varphi_p\varphi_q|\varphi_j\varphi_j\rangle, \end{aligned} \tag{8}$$

$$\begin{aligned} &\langle\varphi_p|K_j|\varphi_q\rangle \\ &\quad = \iint \varphi_p^*(r_1)\varphi_j^*(r_2) g_{12} \varphi_j(r_1)\varphi_q(r_2)\mathrm{d}r_1\,\mathrm{d}r_2 \\ &\quad = \langle\varphi_p\varphi_j|\varphi_j\varphi_q\rangle. \end{aligned} \tag{9}$$

The matrix element of the operator h^{D} is

$$\langle\varphi_p|h^{\mathrm{D}}|\varphi_q\rangle = \int \varphi_p^*(r_1) h^{\mathrm{D}} \varphi_q(r_1)\,\mathrm{d}r_1. \tag{10}$$

The matrix element of the Coulomb–Breit operator is

$$g_{ij} = \frac{1}{r_{ij}} + B_{ij}, \tag{11}$$

where r_{ij} is the distance between the two electrons, and

$$B_{ij} = -\frac{1}{2}\left(\frac{(\vec{\alpha}_i \cdot \vec{\alpha}_j)}{r_{ij}} + \frac{(\vec{\alpha}_i \cdot \vec{r}_{ij})(\vec{\alpha}_j \cdot \vec{r}_{ij})}{r_{ij}^3} \right). \tag{12}$$

In the nonrelativistic approximation the Coulomb–Breit operator is $B_{ij} \equiv 0$.

The two-component spinors are

$$\varphi_i = \begin{pmatrix} \varphi_i^L \\ \varphi_i^S \end{pmatrix} = \begin{Bmatrix} \chi_i^{L+} \\ \chi_i^{L-} \\ \chi_i^{S+} \\ \chi_i^{S-} \end{Bmatrix} \Rightarrow \begin{pmatrix} \sum\limits_{p=1}^{N_L} \chi_p^L c_{pi}^+ \\ \sum\limits_{p=1}^{N_L} \chi_p^L c_{pi}^- \\ \sum\limits_{p=1}^{N_S} \chi_p^S c_{pi}^+ \\ \sum\limits_{p=1}^{N_S} \chi_p^S c_{pi}^- \end{pmatrix}. \tag{13}$$

Atom Molecule

The orbital components φ^S and φ^L in the first approximation are related by

$$\varphi^S \approx \frac{1}{2c}\,\vec{\sigma} \cdot \vec{p}\,\varphi^L, \tag{14}$$

where $\vec{\sigma}$'s are the Pauli matrices (see Eq. (5)).

Atomic Gaussian basis set orbitals are given by [6]

$$\chi_p = N_{\mathrm{a}} x^{n_x} y^{n_y} z^{n_z} \sum_{\alpha_p} A_{\alpha_p}\, \mathrm{e}^{-\alpha_p(x^2+y^2+z^2)}, \tag{15}$$

where N_{a} is the normalization factor, and $n_x + n_y + n_z = l$ is the secondary quantum number. The coefficients A_{α_p} and α_p depend on the atom state and are obtained from the energy minimum condition for the atom [6]:

$$E = \int \Psi^* \left(\sum_i^N h_i^{\mathrm{D}} + \sum_{i>j}^N g_{ij} \right) \Psi\,\mathrm{d}r_1\,\mathrm{d}r_2 \ldots \mathrm{d}r_N, \tag{16}$$

where N is the number of electrons.

The coefficients c_{pi} in Eq. (9) are obtained from the energy minimum condition (Eq. (16)) for the molecule [5, 7].

$$\Psi = \widehat{A}\varphi_1\varphi_2 \cdots \varphi_N \tag{17}$$

is the many-electron antisymmetrical function, and $\widehat{A}$ is the antisymmetrization operator.

3. Electronic structure of the Bi_2S_3 crystal

For the calculation of the electronic structure by the quantum-chemical HF and HFD methods the molec-

Table 1. Bond strengths of the $(Bi_2S_3)_2$ molecule calculated by the HF method at different temperatures. The last column shows the bond strengths for the $(Bi_2S_3)_{10}$ cluster.

Bond	460 K	295 K	130 K	295 K
Bi1–S1	1.46	1.46	1.47	0.92
Bi1–S2	0.81	0.81	0.81	0.72
Bi2–S2	1.02	1.02	1.02	0.60
Bi2–S3	0.93	0.92	0.92	0.94
Bi2–S3	0.64	0.65	0.65	0.23
Bi1–S3	0.33	0.33	0.33	0.13

ular model of the crystal is needed. The model must be a cluster composed from an even number of molecules. The interaction between clusters is assumed to be weak. The crystal structure of Bi_2S_3 is rather favourable for such a model. The structure in the temperature range 130–460 K belongs to the centrosymmetric space group D_{2h}^{16} $(Pbnm)$ [8]. It consists of $[Bi_2S_3]_\infty$ chains parallel to the [001] axis, with strong and short (2.584–2.7439 Å) Bi–S covalent bonds and additionally by much longer Bi–S bonds equal to 3.056 Å. Other interatomic distances between sulphur atoms, within a single chain, are in the region of 3.56–3.67 Å, and may be regarded as weak van der Waals bonds. The pairs of chains (related by the twofold screw axis) are joined (dashed lines in Fig. 1) by longer (2.9656 Å) Bi–S bonds and form ribbons $[[Bi_2S_3]_\infty]_2$. The ribbons connected by still longer (3.035 Å) Bi–S bonds form layers perpendicular to the [010] axis. The structure is quasi-one-dimensional. The structure of the Sb_2S_3 crystal is similar [4].

Figure 1 shows the calculated bond strengths. Within the chains they are of the order of 1.4–0.8 and are shown by solid lines. Between the chains they are of the order of 0.4–0.7 (where the bonds are nonsaturated, Fig. 1(a)) and of 0.2–0.3 (where the bonds are saturated, Fig. 1(b)), and shown by dashed lines. The bond strengths between the ribbons are of the order of 0.1–0.2 (thin lines in Fig. 1(a)). The calculations have shown that the electronic structure depends on the length of the ribbon. Figure 1(b) shows that for the ribbon of ten Bi_2S_3 molecules the bond strengths of the side atoms differ from the bond strengths of the inner atoms because the bonds of the side atoms are broken, i. e. unsaturated. As a result, the bond strengths of the side atoms increase while the ionic charges decrease. Due to this the side atoms become strongly chemically active. The bond strengths and the charges of the inner atoms at different temperatures are shown in Tables 1 and 2. With the increase in temperature the Bi charge decreases due to increase of the interatomic distance [8] and decrease of electronegativity of the S atoms.

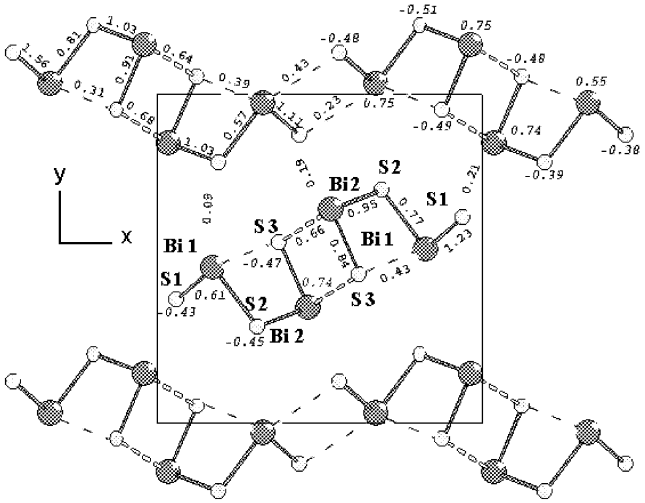

(a)

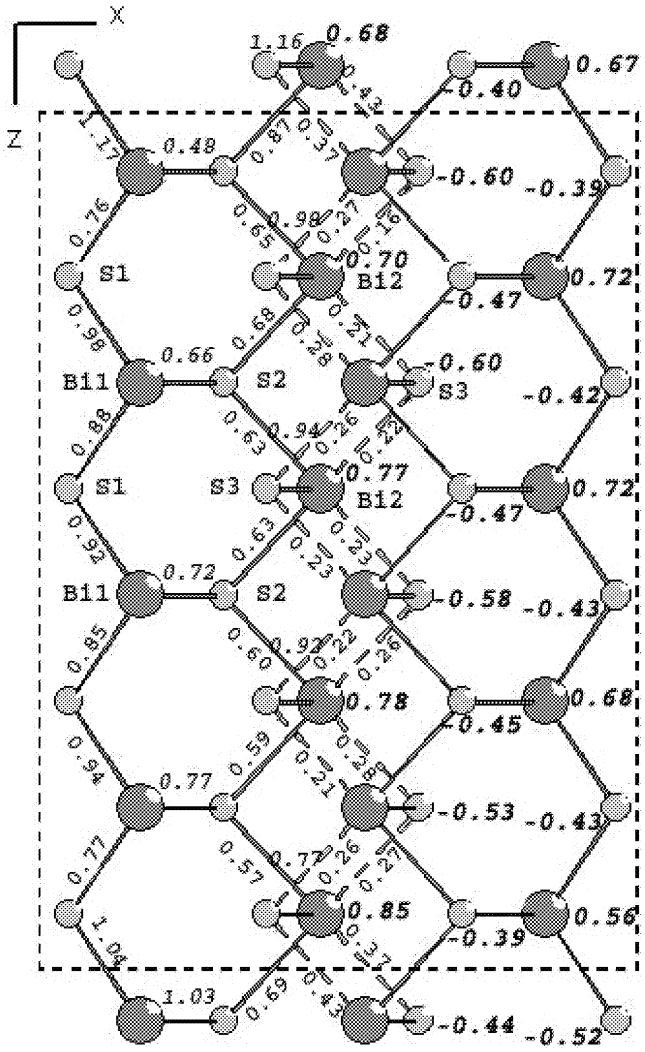

(b)

Fig. 1. The structure of the Bi_2S_3 crystal. Projection of (a) five ribbons on the xy-plane, and (b) of one middle ribbon on the xz-plane. Bond strengths and ionic charges of the $(Bi_2S_3)_{10}$ cluster calculated by the GAMESS program in the 3G basis with all electrons are shown.

Table 2. Mulliken (Mull.) and Löwdin (Löw.) charges of the atoms in the $(Bi_2S_3)_2$ cluster at different temperatures. The last column shows the Mulliken charges for the $(Bi_2S_3)_{10}$ cluster.

Atom	460 K		295 K		130 K		295 K
	Mull.	Löw.	Mull.	Löw.	Mull.	Löw.	Mull.
Bi1	0.53	0.52	0.53	0.52	0.53	0.52	0.72
Bi2	0.73	0.69	0.73	0.69	0.73	0.69	0.77
S1	−0.38	−0.41	−0.38	−0.41	−0.38	−0.41	−0.43
S2	−0.39	−0.37	−0.39	−0.37	−0.40	−0.38	−0.47
S3	−0.48	−0.43	−0.48	−0.43	−0.48	−0.43	−0.58

Table 3. The mean values of the Sb and Bi core level energy (in eV) in a free atom or ion, Sb_2S_3 or Bi_2S_3 molecules, and crystals calculated in the Huzinaga MINI 3G basis and determined experimentally.

Atom	nl	HF, atom	HF, molecule		HFD, atom		HFD, ion A^+		Exp., atom [9]		Exp., crystal [3, 4]	
A			A_2S_3	$(A_2S_3)_2$	nl^+	nl^-	nl^+	nl^-	nl^+	nl^-	nl^+	nl^-
Sb	$3s$	−910.4	−915.0	−915.5					−944		−948	
	$3p$	−787.2	−791.7	−792.1	−794.3	−842.3	−802.9	−850.9	−767	−813	−770	−816
	$3d$	−559.0	−563.4	−563.9	−554.1	−564.0	−562.7	−572.5	−528	−537	−(529–532)	−(538–542)
	$4s$	−162.9	−167.4	−167.6					−153			
	$4p$	−118.9	−123.2	−123.6	−120.8	−129.8	−129.3	−138.3	−99			
	$4d$	−44.0	−48.3	−48.6	−43.7	−45.0	−52.2	−53.5	−33		−(33–35.7)	−(35–37.0)
Bi	$4p$	−688.4	−691.9	−692.3	−707.5	−839.0	−715.7	−847.2	−774	−806		
	$4d$	−481.3	−484.8	−485.2	−465.8	−490.6	−473.9	−498.7	−440	−464	−440	−464
	$4f$	−192.4	−195.9	−196.3	−176.8	−182.5	−184.9	−190.6	−157	−162	−158	−163.5
	$5s$	−148.5	−151.9	−152.3					−161			
	$5p$	−107.9	−111.2	−111.6	−108.2	−133.6	−116.4	−141.7	−93	−119		
	$5d$	−39.7	−42.9	−43.3	−34.6	−37.8	−42.7	−45.9	−24	−27	−25	−28.4

The weak phase transitions at 160 and 410 K also cause small change of the bond strength and charge of atoms. The S3 atoms are the most electronegative, while the Bi2 atoms are more electropositive than the Bi1 atoms. The charge of inner Bi2 atoms is close to the charge of ionized atoms. The Bi_2S_3 crystal can be regarded as composed of two parts: the ionic middle part and the covalent side part of the ribbons. High ionic permittivity $\varepsilon = 100-150$ [1, 2] confirms this conclusion.

4. Analysis of the photoelectron spectra

X-ray photoelectron spectra of Bi_2S_3 and Sb_2S_3 single crystals [3, 4] in the energy range of 0–1400 eV and over a wide temperature range have proven to be temperature dependent. With the increase of temperature the core level energy of Bi and Sb atoms decreases.

As the charge of the inner Bi2 (Table 2) (also of Sb2 [4]) atoms is close to the charge of ionized atoms, the XPS of the crystal may be compared to the XPS of a free A^+ atom. In order to ascertain the advantages of the HFD method, the core level energies of Bi and Sb atoms, as well as of Bi^+ and Sb^+ ions, were calculated and compared with the energies calculated by the HF method and experimental XPS energies. The results are shown in Table 3 and Figs. 2 and 3. The HFD method well evaluates the spin–orbit interaction. The spin–orbit splitting does not depend on the state of the atom: the splitting is the same for both the atom and the ion, e. g., 48 eV for Sb $3p$, 9.9 eV for Sb $3d$; 31.5 eV for Bi $4p$, 5.7 eV for Bi $4f$, 3.2 eV for Bi $5d$ (Table 3). The similar spin–orbit splitting is observed experimentally. The energy obtained by the HF method is not the mean value of the nl^+ and nl^- energy ($l = s, p, d, f$; $l^+ = l + 1/2$; $l^- = l - 1/2$). If the np ($3p$) of the HF coincides with the np^+ of the HFD method and the nd ($3d$) coincides with the nd^- (the lower energy), then the $4f$ energy of the HF method is even lower and coincides with the $4f^-$ state energy of the ionized Bi^+ atom. It means that the orbitals of smaller numbers stronger interact with spin, i. e. more decrease the energy and split the levels.

The HFD method enables one to define exactly the splitting of XPS into two components, nl^+ and nl^-. However, the calculated core level binding energies by both HF and HFD methods are lower up to 40 eV than the experimental values [3, 4]. Very likely it is caused by the relaxation processes, which are not taken into consideration. Nevertheless, both methods show

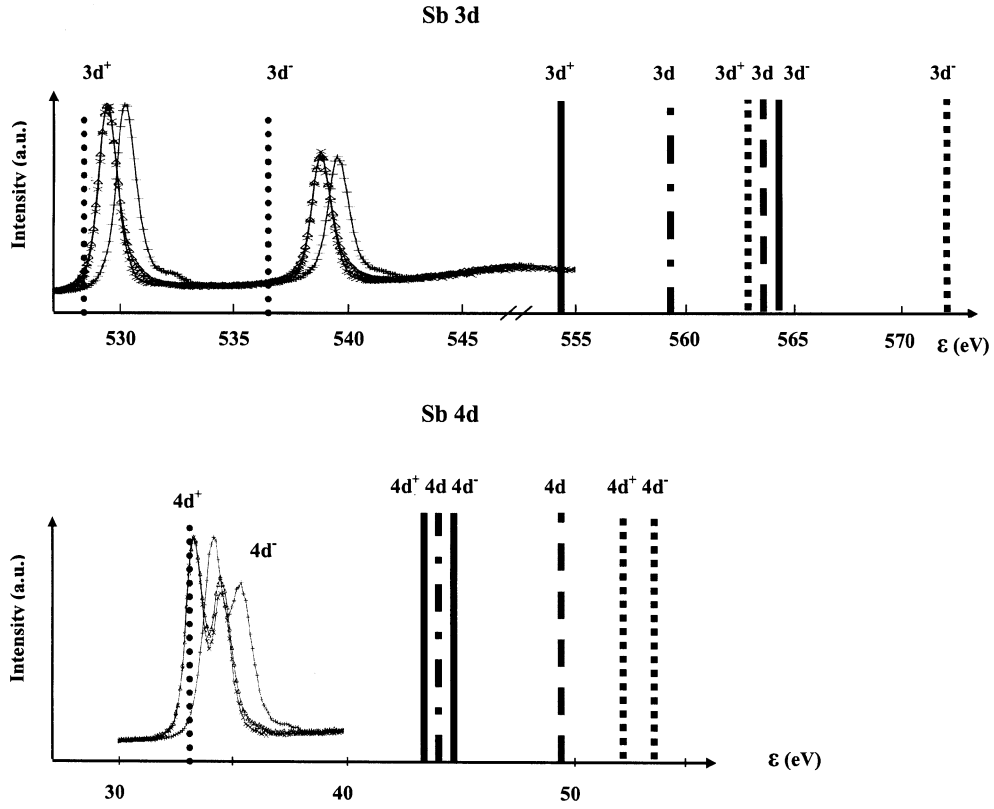

Fig. 2. XPS of Sb $3d$, $3p$, and $4d$. Solid curves: experimental of the Sb_2S_3 crystal at 190 K (right) and 300 K (left) [4]. Round-dotted line: experimental of Sb [9]. Dash-dotted line: theoretical HF of Sb [6]. Thick dashed line: theoretical HF of the $(Sb_2S_3)_2$ crystal [4]. Thick solid line: theoretical HFD of Sb (this work). Square-dotted line: theoretical HFD of Sb^+ (this work).

that the chemical bond formation increases the negative core level binding energy by $\Delta E = 4{-}5$ eV in comparison with the binding energy of a free atom. The qualitatively similar results are obtained experimentally (Table 3).

The energy of atomic orbitals of the free Bi atoms was calculated by the HF method (first column in Table 4) and compared with the energy of the molecular orbitals of Bi_2S_3, $(Bi_2S_3)_2$, $(Bi_2S_3)_4$, $(Bi_2S_3)_6$, and $(Bi_2S_3)_{10}$ molecules. Such a comparison allows evaluating the influence of the Bi_2S_3 chemical bond formation for XPS. It has been found that in the molecules the Bi core level negative energy increases and then remains nearly constant. It means that for the theoretical evaluation of the core level binding energies of XPS the cluster of even one Bi_2S_3 molecule is appropriate. However, such a model would not meet the requirements of symmetry. Table 5 also shows the change of the state energy due to the chemical bond formation. The shift is $\Delta E = (E_{\min} + E_{\max})/2 - E_{\rm a}$, where $E_{\rm a}$ is the energy of the free atom state. In Bi_2S_3 this energy increases by $\Delta E = 3.0{-}4.1$ eV. Contrarily, for S it decreases by $\Delta E = 1.4{-}2.1$ eV in Bi_2S_3 and by $\Delta E = 1.3{-}1.7$ eV in Sb_2S_3. In the Sb_2S_3 molecule, the Sb core level energy increases by $\Delta E = 3.3{-}5.3$ eV. Due to ionicity of the crystals, S atoms attract electrons from Bi and Sb atoms, decrease the screening of the Bi and Sb nuclei, and increase the ionization potential. Sb levels descend lower than Bi levels. It means that Sb is more electronegative, and the Sb_2S_3 crystal is more ionic than the Bi_2S_3 crystal. High ionic permittivity and low frequency of optical phonons [2] confirm this conclusion. The width of the VB p-band in Bi_2S_3 is $\Delta E = 5.1$ eV, and in Sb_2S_3 it is $\Delta E = 5.2$ eV (Table 2).

In the $(Bi_2S_3)_n$ cluster (Table 4), formation of additional chemical bonds widens the level bands: they split into two level groups separated by 1–2 eV. As a result, the negative energy of the Bi core levels decreases in comparison with the energy of two molecules. Bonding of the two Bi_2S_3 molecules (Bi2–S3 dashed bonds in Fig. 1(a)) increases the binding energy by 1.35 eV, while the strong Bi–S bonds in the z-direction (Fig. 1(b)) have the binding energy of 1.77 eV.

With the increase in temperature all the core level energies and the VB decrease (become more positive), as has been observed experimentally [3, 4]. However, due to the observed weak phase transitions in these

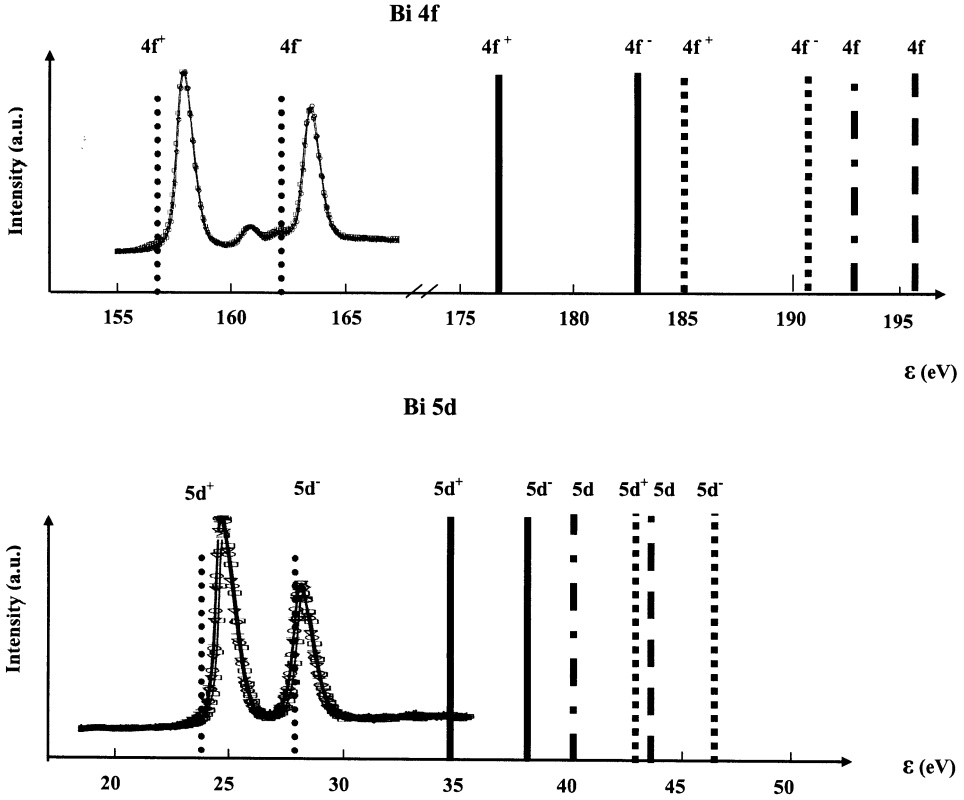

Fig. 3. XPS of Bi $4d$, $4f$, and $5d$. Solid curves: experimental of the Bi_2S_3 crystal [3]. Round-dotted line: experimental of Bi [9]. Dash-dotted line: theoretical HF of Bi [6]. Thick dashed line: theoretical HF of the $(Bi_2S_3)_2$ crystal [3]. Thick solid line: theoretical HFD of Bi (this work). Square-dotted line: theoretical HFD of Bi^+ (this work).

Table 4. The dependence of the mean value of Bi binding energy (in eV) on the number of Bi_2S_3 molecules calculated by the HF method. VB_b is the the bottom and VB_t is the top of the valence band, E_a is the atomization energy needed to decompose the molecule into atoms.

nl	Bi	Bi_2S_3	$(Bi_2S_3)_2$	$(Bi_2S_3)_4$	$(Bi_2S_3)_6$	$(Bi_2S_3)_{10}$
$4s$	−800.8	−804.3	−804.7	−804.5	−804.3	−804.2
$4p$	−688.4	−691.9	−692.3	−692.0	−691.8	−691.8
$4d$	−481.3	−484.8	−485.2	−484.9	−484.7	−484.7
$4f$	−192.4	−195.9	−196.3	−196.1	−195.9	−195.8
$5s$	−148.5	−151.9	−152.3	−152.2	−151.9	−151.9
$5p$	−107.9	−111.2	−111.6	−111.4	−111.2	−111.2
$5d$	−39.7	−42.9	−43.4	−43.3	−43.0	−43.0
VB_b	−15.0	−25.7	−27.1	−28.9	−29.1	−29.1
VB_t	−4.8	−7.8	−8.1	−7.2	−6.7	−6.6
E_a	0	25.9	53.2	104.7	158.6	267.8

crystals [1–4] the solution of the HF equation is not stable enough in all the temperature range.

5. Conclusions

The crystal model for XPS energy calculation of Bi_2S_3-type quasi-one-dimensional crystals is substantiated. The bond strengths between the ribbons along the [001] axis are smaller by one order than the bond strengths within the ribbon. Neglecting the weak interaction of the ribbons, a cluster of two molecules can approximate the crystal for the calculation of XPS. It is found that the length of the ribbon only slightly changes the core level energies. The charge of all atoms in the $(Bi_2S_3)_{10}$ or $(Sb_2S_3)_{10}$ cluster is different, i. e. in Bi_2S_3 it is $Bi2^{0.77}Bi1^{0.74}S1^{-0.43}S2^{-0.47}S3^{-0.58}$, while in Sb_2S_3 it is $Sb2^{0.83}Sb1^{0.75}S1^{-0.46}S2^{-0.51}S3^{-0.62}$.

Table 5. Core level energies $E_{\rm cl}$ (in eV) of Bi, Sb, and S atoms and their shifts ΔE in $(Bi_2S_3)_2$ and $(Sb_2S_3)_2$ clusters calculated by the RF method in the Huzinaga MINI basis.

Atom	nl	$E_{\rm cl}$	$E_{\rm min}$	ΔE	$E_{\rm max}$
$(Bi_2S_3)_2$, 130 K					
Bi	$1s$	−81217	−81222	−4.1	−81220
	$2s$	−13918	−13923	−4.0	−13922
	$2p$	−13398	−13403	−4.0	−13402
	$3s$	−3403	−3407	−3.9	−3406
	$3p$	−3153	−3157	−3.9	−3156
	$3d$	−2685	−2690	−3.9	−2689
	$4s$	−800.8	−805.5	−3.9	−804.0
	$4p$	−688.4	−693.0	−3.8	−691.5
	$4d$	−481.4	−485.9	−3.9	−484.4
	$4f$	−192.6	−197.1	−3.9	−195.6
	$5s$	−148.6	−153.0	−3.7	−151.6
	$5p$	−107.9	−112.4	−3.7	−110.8
	$5d$	−39.8	−44.2	−3.6	−42.5
	$6s$	−15.0	−19.2	−3.0	−16.7
	$6p$	−4.6			
S	$1s$	−2484	−2483	1.8	−2480
	$2s$	−242.4	−242.4	1.4	−239.6
	$2p$	−178.3	−178.4	1.4	−175.4
	$3s$	−27.0	−27.1	2.1	−22.7
	$3p$	−10.3			
VB (p-band)			−13.2		−8.1
$(Sb_2S_3)_2$, 120 K					
Sb	$1s$	−29373	−29379	−5.3	−29377
	$2s$	−4468	−4474	−5.1	−4472
	$2p$	−4175	−4181	−5.1	−4180
	$3s$	−910.4	−916.1	−4.9	−914.6
	$3p$	−787.2	−792.8	−4.8	−791.3
	$3d$	−559.0	−564.7	−4.9	−563.2
	$4s$	−162.9	−168.2	−4.6	−166.8
	$4p$	−118.9	−124.3	−4.6	−122.8
	$4d$	−44.0	−49.4	−4.5	−47.8
	$5s$	−15.1	−19.7	−3.3	−16.9
	$5p$	−3.9			
S	$1s$	−2484	−2483	1.7	−2481
	$2s$	−242.4	−242.2	1.3	−239.9
	$2p$	−178.3	−178.2	1.3	−175.8
	$3s$	−27.0	−27.5	1.7	−23.1
	$3p$	−10.3			
VB (p-band)			−13.4		−8.2

Therefore, the Sb_2S_3 crystal is more ionic than Bi_2S_3. The charge of atoms in the middle of the ribbon is higher than that of side atoms. The HF method does not take into account the spin–orbit interaction and thus gives no spin–orbit splitting of XPS. However, the HFD method gives the proper experimentally observed spin–orbit splitting of the core level energies. Atomic orbitals of a lower quantum orbital number stronger interact with spins. Both the HF and HFD methods neglect relaxation processes and give the core level energies from several to several dozen eV lower than the experimental XPS values. The core level energy calculated by the HF method is not the average of l^+ and l^- values calculated by the HFD method. Nevertheless, HF and HFD methods provide invaluable tools in assigning experimental XPS.

References

[1] A. Kajokas, J. Grigas, A. Brilingas, J. Banys, K. Lukaszewicz, A. Audzijonis, and L. Žygas, Origin of anomalies of physical properties in Bi_2S_3 crystals, Lithuanian J. Phys. **39**, 45–53 (1999).

[2] J. Grigas, *Microwave Dielectric Spectroscopy of Ferroelectrics and Related Materials* (Gordon & Breach, Amsterdam, 1996) p. 336.

[3] J. Grigas, E. Talik, and V. Lazauskas, X-ray photoelectron spectra and electronic structure of Bi_2S_3 crystals, Phys. Status Solidi B **232**, 220–230 (2002).

[4] J. Grigas, E. Talik, and V. Lazauskas, X-ray photoelectron spectroscopy of Sb_2S_3 crystals, Phase Transitions **75**, 323–337 (2002).

[5] L. Visscher, O. Visser, P.J.C. Aerts, H. Merenga, and W.C. Nieuwpoort, Relativistic quantum chemistry: The MOLFDIR program package, Comput. Phys. Commun. **81**, 126–144 (1994).

[6] *Gaussian Basis Sets for Molecular Calculations*, ed. S. Huzinaga (Elsevier, Amsterdam/Oxford/New York/ Tokyo, 1984) p. 426.

[7] M.W. Schmidt, K.K. Baldrige, J.A. Boatz, S.T. Elbert, M.S. Gordon, J.H. Jensen, S. Koseki, N. Matsunaga, K.A. Nguyen, S.J. Su, T.L. Windus, M. Dupuis, and J.A. Montgomery, General atomic and molecular electronic structure system, J. Comput. Chem. **14**, 1347–1363 (1993).

[8] K. Lukaszewicz, J. Stepien–Damm, A. Pietraszko, A. Kajokas, and J. Grigas, Crystal structure, thermal expansion, dielectric permittivity and phase transition of Bi_2S_3, Polish J. Chem. **73**, 541–546 (1999).

[9] J.F. Moulder, W.F. Stickle, P.E. Sobol, and K.D. Bomben, *Handbook of Photoelectron Spectroscopy* (Physical Electronics, Minnesota, USA, 1995).

CHEMINIŲ RYŠIŲ ĮTAKA Sb IR Bi RÖNTGEN'O FOTOELEKTRONŲ SPEKTRO POSLINKIAMS Sb_2S_3 IR Bi_2S_3 KRISTALUOSE

V. Lazauskas [a], V. Nelkinas [a], J. Grigas [b]

[a] *Vilniaus pedagoginis universitetas, Vilnius, Lietuva*
[b] *Vilniaus universitetas, Vilnius, Lietuva*

Santrauka

Straipsnyje Hartree ir Foko (HF) bei Hartree, Foko ir Dirac'o (HFD) metodais kvazivienmačio kristalo kekės modeliu (1 pav.) apskaičiuotas Sb_2S_3 ir Bi_2S_3 kristalų vienelektronių energijų lygmenų spektras, kuris pagal Koopmans'o teoremą atitinka Röntgen'o fotoelektronų spektro (FES) energijos vertes. Gautieji rezultatai palyginti su atskirų atomų bei kristalų eksperimentiniais FES (3 lentelė). Apskaičiuoti ir eksperimentiniai kristalo spektrai yra keliais eV pasislinkę, lyginant su laisvo atomo FES (4 ir 5 lentelės), tačiau teorinės absoliutinės FES vertės, apskaičiuotos tiek HF, tiek HFD metodu, yra keliasdešimt eV mažesnės (žr. 2 ir 3 pav.), tik HFD metodu gana tiksliai įvertinamas lygmenų suskilimas į $l \pm 1/2$ sandus (3 lentelė). Skaičiavimais patvirtinta kristalų joninė ryšių sandara, Sb ir Bi krūviai artimi 1, o Sb yra elektroteigiamesnis negu Bi (žr. 1 ir 2 lenteles).